Hindawi
Journal of Sensors
Volume 2019, Article ID 1359853, 13 pages
https://doi.org/10.1155/2019/1359853

Research Article

Damage Quantification in Concrete under Fatigue Loading Using Acoustic Emission

Zhi Shan,[1,2,3] **Zhiwu Yu**,[1,2,3] **Xiao Li**,[1,2] **and Ying Xie**[1,2]

[1]*School of Civil Engineering, Central South University, 68 South Shaoshan Road, Changsha 410075, China*
[2]*National Engineering Laboratory for High Speed Railway Construction, 68 South Shaoshan Road, Changsha 410075, China*
[3]*Engineering Technology Research Center for Prefabricated Construction Industrialization of Hunan Province, Central South University, 68 South Shaoshan Road, Changsha 410075, China*

Correspondence should be addressed to Zhiwu Yu; zhwyu@csu.edu.cn

Received 24 May 2019; Accepted 17 July 2019; Published 3 November 2019

Academic Editor: Jerome Rossignol

Acoustic emission (AE) is an effective nondestructive evaluation method for assessing damage in materials; however, few works in the literature have focused on one quantification method of damage in concrete under fatigue loading by using AE for characterizing the entire three main deterioration behaviors simultaneously. These deterioration behaviors include Young's modulus degradation, fatigue total strain, and residual strain development. In this work, an AE quantification method of fatigue damage in concrete was developed, by combining AE and a fiber bundle-based statistical damage model (fiber bundle-irreversible chain model). By establishing a relationship between normalized AE counts and the damage variable based on the fiber bundle-irreversible chain model, the method was proposed. Additionally, this method was verified against the experimental results. It is able to capture the mechanisms of damage accumulation and characterize the three deterioration behaviors simultaneously.

1. Introduction

Acoustic emission (AE), as a nondestructive evaluation and diagnostic technique, has been developed for more than three decades [1–6]. By considering the highly sensitively detecting results of active microscopic events (e.g. microcrack initiation and propagation) in materials provided by AE, it is widely adapted for materials research [1–9]. In detail, by applying AE sensors on certain materials, the propagated elastic waves produced by the abovementioned events are detected; further, the location and state of the damage/crack are determined [7–9].

The understanding of deterioration behaviors for concrete under fatigue loads is essential for the assessment and analysis of relevant structures. Specifically, those deterioration behaviors consist of Young's modulus degradation, fatigue total strain, and residual strain development, which further cause an abrupt failure of the structures. For example, the repeated train loading on high-speed railway concrete structures typically results in the safety problems by the influence of such deterioration. Recently, there are significant advancements in AE techniques on the continuous monitoring for materials under fatigue loading [10–12]. For example, Kahirdeh et al. [11] proposed a parametric approach to estimating acoustic information entropy and relative entropy of aluminum alloys by examining the acoustic signal. In addition, the researchers also observed the relationship between the evolutions of those variables and the fatigue damage concerning the hardness change, respectively.

However, few works in the literature have focused on one quantification method of damage in concrete under fatigue loading by using AE for characterizing the entire three deterioration behaviors simultaneously. Specifically, most contributions only considered the experimental investigations on the empirical relationship between a single deterioration behavior and a certain AE parameter [13–19]. For instance, Wang et al. [15] conducted the comparison on the fatigue properties among plain concrete, rubberized concrete, and polypropylene fiber-reinforced rubberized concrete by applying AE, and the results showed a linear

correlation between the AE counts and the residual strain for plain and rubberized concrete, respectively. Additionally, based on a AE rate process theory, Ohtsu and Watanabe [17], Suzuki and Ohtsu [18], and Dai and Labuz [19] defined a probability density function $f(V)$ of AE events, which was dependent on the stress level $V = \sigma/f_c$ for investigating the evolution of $f(V)$ (where σ and f_c denotes the stress and strength, respectively) on concrete. Furthermore, Ohtsu and Watanabe [17] and Suzuki and Ohtsu [18] observed the relationship between a key parameter and a damage variable for concrete. In detail, the key parameter was obtained by fitting the evolution of $f(V)$ with a hyperbolic function, and the damage variable was introduced by considering the stiffness degradation.

For nearly one hundred years, a class of simple statistical damage models, namely, fiber bundle models (FBMs), have received growing attention in both the physics and engineering communities [20–24], due to their deceptively simple appearance coupled with an outstanding richness of mechanical behaviors. The classical FBMs were developed to characterize the progressive elastic deformation damage relating to Young's modulus degradation, which is represented by the continuously breaking of fibers. However, it is unable to characterize the development of irreversible/residual strains in materials. The development of irreversible/residual strain is a significant property for describing the fatigue behaviors in the sense of material behavior. Therefore, in order to characterize such property, the irreversible deformation element was introduced into the classical FBMs [24–30]. Specifically, the irreversible deformation element is able to simulate the development of irreversible strains represented by the progressive fracture of elements. These models [24–30] were developed to characterize both the progressive elastic deformation damage resulted from the micro mode-I crack process and the irreversible/residual deformation damage produced by serials of types of cracks. The types of cracks are generally distinguished as follows: the irreversible opening of mode-I crack due to locking mechanisms of crack faces [31], the irreversible sliding-like of mode-II crack (not mode-II microcracks) due to toughness of crack faces [32, 33], the irreversible-frictional sliding over crack surface [34, 35], the irreversible cracking of fracture process zone [27, 36], the irreversible mode-II microcracks [37, 38], and other cracking mechanisms [39, 40]. It is verified that the irreversible deformation element is able to effectively model the development of the irreversible/residual strains in the materials [24–30]. Precisely, the fibers and irreversible deformation elements with random thresholds are introduced in FBMs for modelling the events of microcracking in the materials, which were detected by AE sensors.

Furthermore, the fiber bundle-irreversible chain model (BCM, the expression "plastic chain" [41] is corrected by "irreversible (deformation) chain" in this work based on the literature [27, 31–40]) was developed based on the FBMs for describing the abovementioned deterioration behaviors of quasibrittle materials under fatigue loading during the lifetime. This model was verified to be able to capture the major microscopic mechanisms of the deterioration behaviors against the experimental results [41]. Recently, Sa'nchez-Molina et al. [42] proposed a stochastic model for modelling the soft tissue failure under monotonic loading by combining the FBM and AE. The relationship between fiber failure number and AE counts and the relationship between damage variable and AE cumulative energy were both examined. Although this method only considered the relationship between AE parameters and stress response of the material under monotonic loading, it provides us a new approach to studying the deterioration behaviors under fatigue loading by using AE.

In this work, a method of quantification of damage in concrete under fatigue loading is proposed based on AE and BCM. This method is aimed at characterizing the three deterioration behaviors simultaneously. The outline of the work is as follows: after a brief introduction of the BCM relating to the damage accumulation, the quantification method of fatigue damage in concrete is developed, and subsequently, this method is verified by comparing the predictions with experimental results.

Note that this work only focuses on the damage and AE responses of the concrete materials (i.e., the representative volume elements (RVEs)) due to the sophisticated behaviors under fatigue loading, although a number of works have been contributed by researchers concerning that of reinforced concrete structures. Considering that the materials' behaviors are essential for further analysis of the mechanical behaviors of structures, a great number of studies have been already conducted in the literature [14, 15, 17, 19, 28, 29, 31, 42, 43]. In addition, the damages of concrete structures subjected to mode-I, mode-II, and mixing mode loading were classified by using AE [3]. However, the feasibility of such method is probably limited for concrete material due to the differences between the damage behaviors of structures and materials caused by different scales. In the perspective of material, concrete mainly consists of three constituents: the cement matrix (a microdefect-filled material), the aggregates, and the interface between the matrix and aggregates (transition halo, the weakest zone in concrete, which is highly oriented because of wall effects). Therefore, it causes concrete containing full of flaws and preexisting cracks from nanoscale to mesoscale and results in the complex damage behaviors in the material; e.g., when the concrete material is subjected to uniaxial tension, there are different modes of cracks generated during the loading. The further work concerning the damage and AE responses of reinforced concrete structures will be conducted by the authors' research team.

2. Fiber Bundle-Irreversible Chain Model with Damage Accumulation

The BCM with the damage accumulation was developed based on the statistical methods, namely, FBMs. This model is aimed at characterizing the deterioration behaviors of quasibrittle material under fatigue loading [41]. The main methodology of the theoretical method is briefly introduced.

The BCM [41] was composed of a bundle of parallel linearly elastic fibers with the same Young's modulus E_0 and a chain of linked perfectly irreversible deformation elements with the same Young's modulus $1000E_0 >> E_0$. Each irreversible deformation element was presumed to obtain the same irreversible strain $r0$ after reaching its threshold, driven by the effective stress [30, 41]. After each fiber breaking event, the load of the failed fiber was assumed to be equally redistributed over the intact ones in the bundle in an equal-load sharing pattern without consideration of their distance from the failure point [20–30]. Under fatigue loading, the fibers progressively fail due to breaking and the irreversible deformation elements gradually fracture due to the abovementioned cracks [27, 31–40]. Specifically, two mechanisms (elastic and irreversible deformation damage accumulation) are considered as follows [41]:

(i) Fiber i $(i = 1, \cdots, n)$ fails instantaneously at time t when the strain $\varepsilon_i(t)$ reaches its breaking threshold $\varepsilon_{\text{th},i}(t)$

(ii) Irreversible deformation element j $(j = 1, \cdots, n)$ fractures instantaneously at time t when the strain $\varepsilon_j(t)$ (corresponding to the effective stress $\sigma_{\text{eff},j}(t)$) reaches its fracturing threshold $\varepsilon_{\text{th},j}(t)$

The system BCM experiences an accumulation process of both types of damages during the lifetime; hence, the system, rather than the individual fiber or irreversible deformation element, is endowed with a memory of the load history. Consequently, this methodology introduces a scaling method for characterizing the deterioration behaviors of concrete in time space [41].

By using the statistical theory [20–30], the accumulated elastic and irreversible deformation damage $d(t)$ and $r(t)$ up to time t can be calculated by integrating the time t over the entire failures of fibers and fractures of irreversible deformation elements, respectively [41]:

$$\begin{aligned} d(t) &= D_d(t) = \int_0^i P_d\left(t'\right) dt', \\ r(t) &= D_p(t) = \int_0^i P_p\left(t'\right) dt', \end{aligned} \tag{1}$$

where t' denotes the time and $P_d(t)$ and $P_p(t)$ and $D_d(t)$ and $D_p(t)$ denote the probability densities and the cumulative distributions of the breaking thresholds $t_{\text{th},i}$ and the fracture thresholds $t_{\text{th},j}$ in time space, corresponding to the breaking thresholds $\varepsilon_{\text{th},i}(t)$ and the fracturing thresholds $\varepsilon_{\text{th},j}(t)$ in total strain space, respectively [41]. Furthermore, for describing the nonlinear behavior of concrete which coupled both the accumulated elastic and irreversible deformation damages, the total damage variable $dr(t)$ up to time t can be obtained by integrating over the entire history of both fiber failures and irreversible deformation element fractures [41], such that

$$dr(t) = d(t) + r(t) = D(t) = \int_0^i P\left(t'\right) dt', \tag{2}$$

where $P(t)$ denotes the probability density coupling with fiber failures and irreversible deformation element fractures and $D(t)$ denotes the cumulative distribution of thresholds coupling with fiber failures and irreversible deformation element fractures in time space (i.e., thresholds t_{th}), relative to the thresholds in total strain space (i.e., threshold $\varepsilon_{\text{th}}(t)$).

Therefore, the constitutive relationship of the BCM under a constant maximum loading $\sigma_{\max}$ was obtained such that [41]

$$\sigma_{\max} = [1 - dr(t)] \cdot E_0 \cdot \varepsilon(t). \tag{3}$$

To characterize the evolution of the total damage variable conveniently, the parameters dr_{t1} and dr_{tNf} were introduced [41] by using an analytical method based on the fatigue failure surface concept [44, 45] as follows:

$$dr(t) = dr_{t1} + \left(dr_{tNf} - dr_{t1}\right) \cdot dr_0(t), \tag{4}$$

where dr_{t1} and dr_{tNf} denote the total damage variable after the time of first loading cycle and at the time to fatigue failure, respectively, which are affected by $\sigma_{\max}$ or the stress level $S = \sigma_{\max}/f_c$ (f_c denotes the strength); they are calibrated by the analytical method based on the fatigue failure surface concept [44, 45], and $(dr_{tNf} - dr_{t1})$ is in the interval $0 < (dr_{tNf} - dr_{t1}) < 1$, varied with different stress levels S; dr_0 denotes the normalized total damage variable; it is a parameter by normalizing $dr(t)$ from dr_{t1} to dr_{tNf} and defined by the equation $dr_0(t) = [dr(t) - dr_{t1}]/(dr_{tNf} - dr_{t1})$, in the interval $0 \le dr_0 \le 1$.

3. Acoustic Emission Quantification of Fatigue Damage

3.1. Relationship between AE Parameter and Fatigue Damage. In AE, several parameters are usually evolved including amplitude, duration, energy, threshold, frequency, rise time, and counts. Among these parameters, the amplitude, energy, and counts were typically applied to investigate the damage of materials. Figure 1 illustrates that all the counts (C), accumulated energy (Ae), energy rate, and amplitude experience a three-stage process during the lifetime of typical concrete under fatigue loading. By observing the relationship between the AE parameters and fatigue damage, the following are found:

(1) By using a certain modification method, AE counts are able to characterize the evolution of damage in materials under fatigue. The count is defined as the number of times the AE signal amplitude exceeds a given threshold during experiments. The reasons

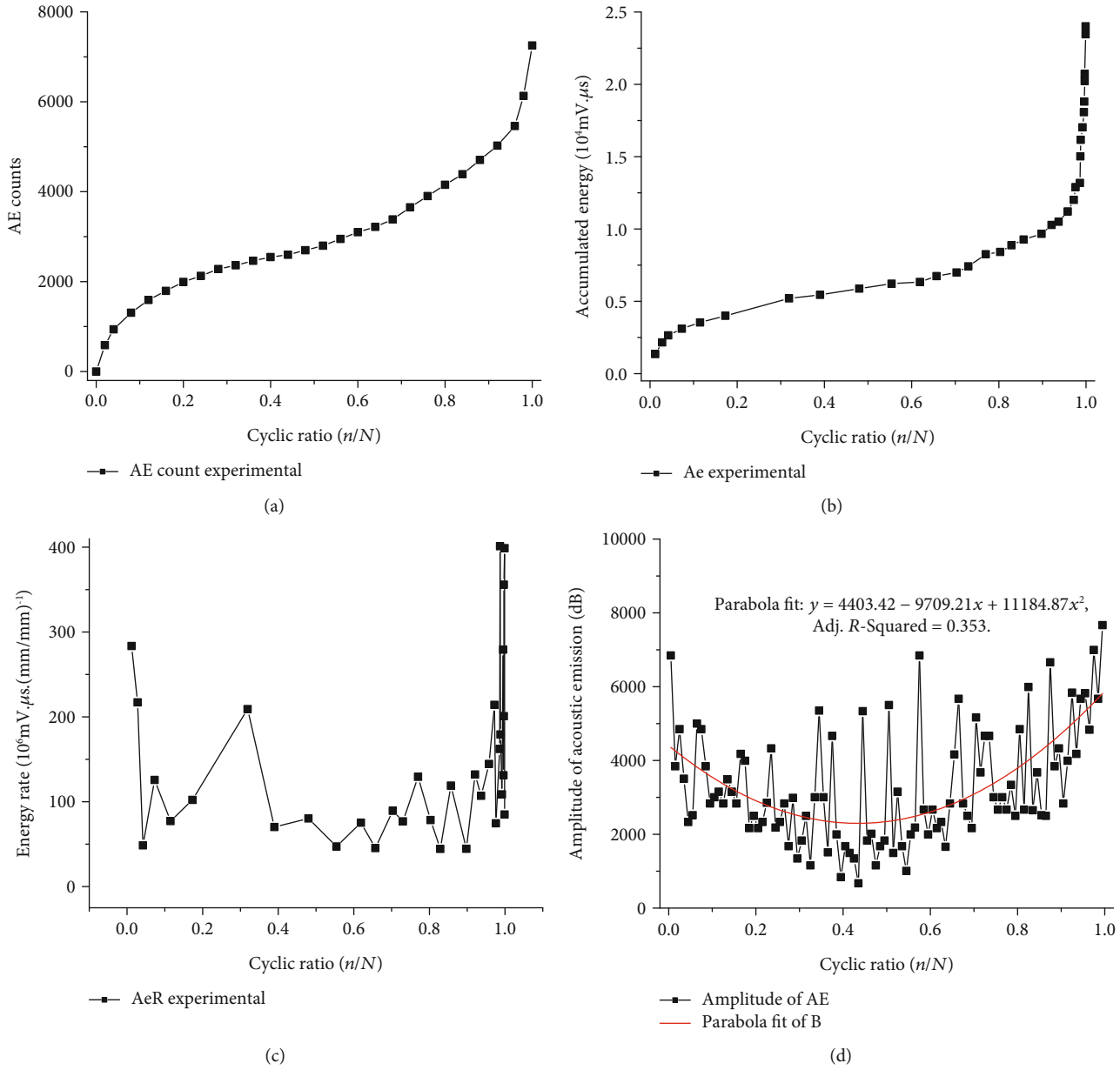

Figure 1: Typical experimental results of AE for concrete during lifetime [12]. (a) AE counts, (b) accumulated AE energy, (c) AE energy rate, and (d) AE amplitude.

are concluded as follows: initially, the application of AE counts on material characterization is verified. Although several researchers regarded the AE counts as an unreliable indicator of damage, it is considered the most direct response to the microstructural variation in materials [46]. A number of works on studying the relationship between fatigue behaviors and AE responses of materials have been conducted by using AE counts [15, 17, 42, 46–55]. Based on AE counts, the literature [56, 57] defined a new AE parameter, average frequency (AF), for fracture mode classification. Moreover, Figure 1(a) and other literatures [15, 47, 48] show the evolution trend of AE counts and the typical fatigue strain development are similar to each other. In addition, it is presumed that the AE counts are in certain correlation with the number of failure/fracture events in the BCM. Although it is found that a large variation of AE counts could be resulted by changing a threshold by only a small proportion, in this work, after using a certain modification method (e.g., normalization) on AE counts, the resulted parameter relative to AE counts is undergoing a stable evolution process.

It is noted in the literature [58] that a quiet time zone of AE counts appeared at the beginning during the lifetime. The causes are concluded as follows: firstly, due to the significant low value of the maximal fatigue load compared with the peak static load of the specimen at the beginning of the lifetime, the driven loading for the microcrack initiation is

insufficient. For example, the maximal fatigue loading in the literature [58] was only 0.04~0.11 times to the peak static load at the beginning. Secondly, it is presumed that during the beginning of loading cycles, the behaviors of crack initiation and propagation are similar to that under static loading (defined as the quasistatic effect in this work). The quasistatic effect gradually decreases with the growth of the cycle number and recedes when approaching the second stage of lifetime.

It is also noted that the decline of an application of AE counts [15, 42, 46–55], even those with certain modifications [17, 18], will result in a subsequent decline of the application of average frequency (AF) and others [56, 57]. The reason is concluded that, if a large variation of AE counts could be caused by changing a threshold by only a small proportion as one who claims, while only a relatively small variation of AE duration could be generated by the mentioned changing, the average frequency (AF) could obtain a larger variation subsequently.

Furthermore, note that the well-accepted AE methods [17, 18] encourage this work to employ AE counts to quantify fatigue damage of concrete by normalizing the counts. The evolution trend of AE counts dependent on the static stress level (i.e., relative static stress magnitude) ensures a stable status for estimating the rate of the trend; therefore, the evolution trend dependent on the load cycle number is presumed to ensure another stable status for characterizing the accumulation process. The evolution trend of AE counts [17, 18], rather than the counts themselves, may eliminate passive influence of the threshold-caused variation abovementioned; it is also assumed to be effective for the evolution trend of normalized AE counts in this work.

(2) The evolution of accumulated AE energy is different from that of damage in materials under fatigue. In detail, the energy dissipation is usually included that resulted from mode-I crack initiation/growth (modeled by fiber failure) and an irreversible deformation fracture initiation/growth (modeled by irreversible deformation element fracture). Precisely, the amounts of the energy dissipation resulted from those types of microscopic events are usually different from each other. Moreover, it is found that there are significant variations in energy dissipation resulted from a single mode-I crack initiation/growth event (modeled by fiber failures and named microfailures in the literature [42]) in different time.

(3) Both the AE energy rate and AE amplitude typically undergo a three-stage process. It is presumed that those parameters are able to reflect the microscopic crack behaviors in a certain degree. However, they were not considered the most direct indicators of the microscopic events in materials [46].

Therefore, the normalized AE counts, rather than AE counts, are considered the essential parameter for the quantification of fatigue damage in this work.

3.2. Fatigue Total Damage Variable Definition Using Normalized AE Counts. In order to quantify the fatigue damage, the following steps are suggested to be conducted by using the normalized AE counts.

In a perfect condition, since each microscopic event is detected by the sensor and counted once, the AE counts are equal to the number of microscopic events in each cycle during the lifetime. Therefore, the total damage variable is defined by adopting the normalized AE counts by casting in the form of equation (4) as follows:

$$\overline{dr_{\mathrm{AE}}}(t) = dr_{t1} + \left(dr_{tNf} - dr_{t1}\right) \cdot \overline{dr_{0,\mathrm{AE}}}(t), \tag{5}$$

where $\overline{dr_{0,\mathrm{AE}}}(t)$ denotes the normalized total damage variable computed by using the normalized AE counts in the perfect condition. Moreover, the total damage variable obtained by count is equal to that in equation (4) based on BCM, such that

$$\overline{dr_{\mathrm{AE}}}(t) = dr(t). \tag{6}$$

However, during the normal AE experiments, the count generally is not equal to the number of microscopic events in each cycle. The reason can be concluded as in real experiment, one counted signal is incapable of reflecting a single breaking/fracture event in materials [42]. Specifically, a group of breaking/fracture events may only generate only one counted signal, which means that a number of breaking/-fracture events are missed during the counting process. In addition, the amplitude of the signal is generally found to be lower than the threshold determined empirically, in which it is attributed to the influences of the constraint condition near the zone of certain microevents and the AE sensors are installed too far from the locations where the microevents occurred [3].

Hence, due to the misestimation based on the AE counts, the total damage variable based on AE is defined by considering a correction as follows:

$$dr_{\mathrm{AE}}(t) = \overline{dr_{\mathrm{AE}}}(t) - dr_{\mathrm{AE},C}(t), \tag{7}$$

where $dr_{\mathrm{AE},C}(t)$ denotes the correction of the total damage variable based on AE. Additionally, based on equations (4) and (5), the expression of the variable $dr_{\mathrm{AE}}(t)$ is further simplified such that

$$dr_{\mathrm{AE}}(t) = dr_{t1} + \left(dr_{tNf} - dr_{t1}\right) \cdot dr_{0,\mathrm{AE}}(t), \tag{8}$$

where $dr_{0,\mathrm{AE}}(t)$ denotes the normalized total damage variable computed by using AE counts, within the interval $0 \le dr_{0,\mathrm{AE}}(t) \le 1$.

3.3. Quantification of Fatigue Damage Using AE. In order to quantify the fatigue damage by applying normalized AE counts, based on equations (4) and (6)–(8), both parameters $dr_{0,\mathrm{AE}}(t)$ and $dr_{\mathrm{AE},C}(t)$ are needed to be estimated initially. The parameter $dr_{0,\mathrm{AE}}(t)$ is proposed to be defined by normalizing the AE counts $C(t)$ from the first loading cycle $C(t_1)$ to

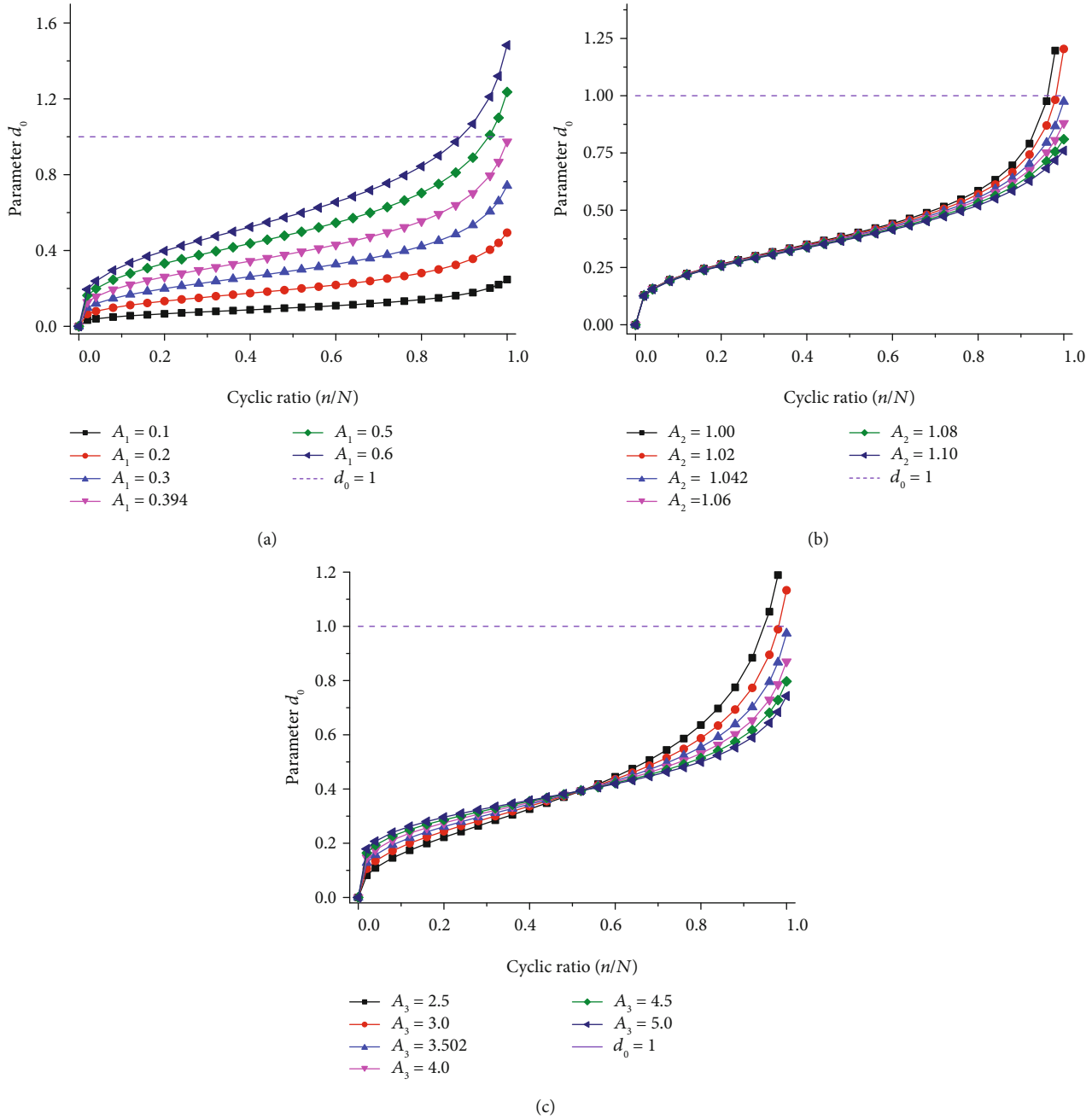

FIGURE 2: Analyzed results of parameter effects on the evolution of normalized damage variable (d_0) for concrete during lifetime. (a) Effect of parameter A_1 by setting $A_2 = 1.042$ and $A_3 = 3.502$. (b) Effect of parameter A_2 by setting $A_1 = 0.394$ and $A_3 = 3.502$. (c) Effect of parameter A_3 by setting $A_1 = 0.394$ and $A_2 = 1.042$.

the cycle of fatigue failure $C(t_{Nf})$, such that

$$dr_{0,\mathrm{AE}}(t) = \frac{C(t) - C(t_1)}{C(t_{Nf}) - C(t_1),} \tag{9}$$

where the AE counts $C(t)$ are computed by experimental results (e.g., Figure 1(a) [15]). For simplicity, an equation for describing the evolution of the normalized total damage variable $dr_{0,\mathrm{AE}}(t)$ is suggested in this work as follows:

$$dr_{0,\mathrm{AE}}(t) = A_1 \left(-\frac{t}{t - A_2} \right)^{1/A_3}, \tag{10}$$

where A_1, A_2, and A_3 denote the parameters relating to the damage behaviors due to microscopic crack initiation/-growth, which can be calibrated by fitting the experimental results.

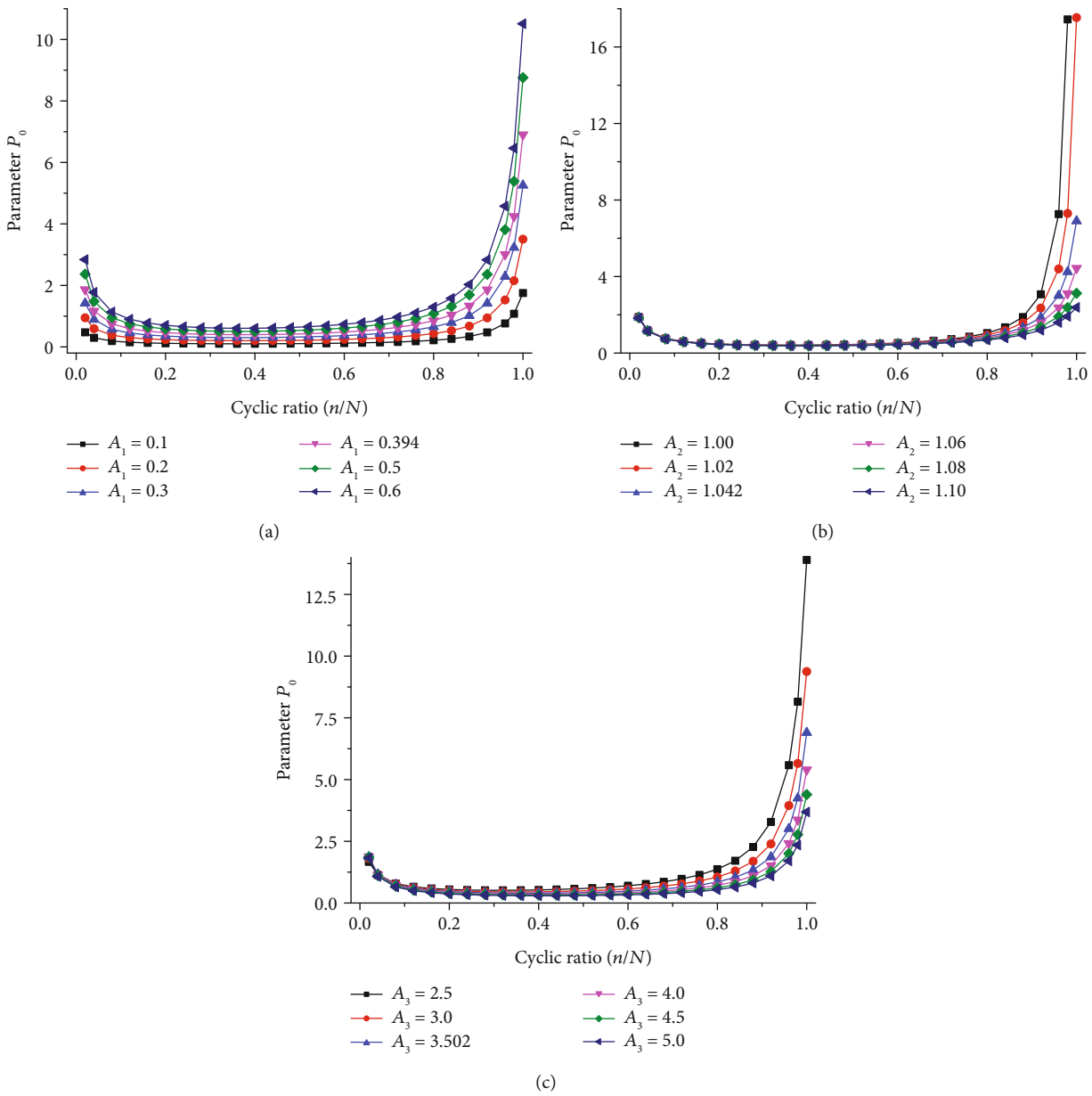

FIGURE 3: Analyzed results of parameter effects on the rate of normalized damage variable (P_0) for concrete during lifetime. (a) Effect of parameter A_1 by setting $A_2 = 1.042$ and $A_3 = 3.502$. (b) Effect of parameter A_2 by setting $A_1 = 0.394$ and $A_3 = 3.502$. (c) Effect of parameter A_3 by setting $A_1 = 0.394$ and $A_2 = 1.042$.

Moreover, Figures 2 and 3 obtain the analysis of parameter effects on the evolution of the normalized damage variable d_0 and the rate of the normalized damage variable P_0. The figures illustrate that as a scale factor, parameter A_1 affects the magnitude of both variables d_0 and P_0 during the whole lifetime. In detail, the higher parameter of scale factor A_1 results in the higher magnitude of both variables. In addition, parameter A_2 mainly affects variables d_0 and P_0 during the last stage of the lifetime, in which the lower the parameter the higher the magnitude of both variables. Furthermore, parameter A_3 also contributes to the effects on variables d_0 and P_0, in which the lower the parameter the higher the rate of the magnitude of both variables during the second stage of lifetime. Therefore, the proposed relationship (equation (10)) is able to characterize the three-stage fatigue damage evolution of concrete by adopting certain calibration of the parameters.

Additionally, considering the misestimation based on the AE counts in Section 3.2, the parameter $dr_{\mathrm{AE,C}}(t)$ is suggested to be expressed by the equation such that

$$dr_{\mathrm{AE,C}}(t) = A_4 \cdot dr_{\mathrm{AE}}(t) + A_5 \cdot dr_{\mathrm{AE}}^2(t), \tag{11}$$

where A_4 and A_5 denote the parameters relating to the misestimation based on the AE counts, which can be calibrated by

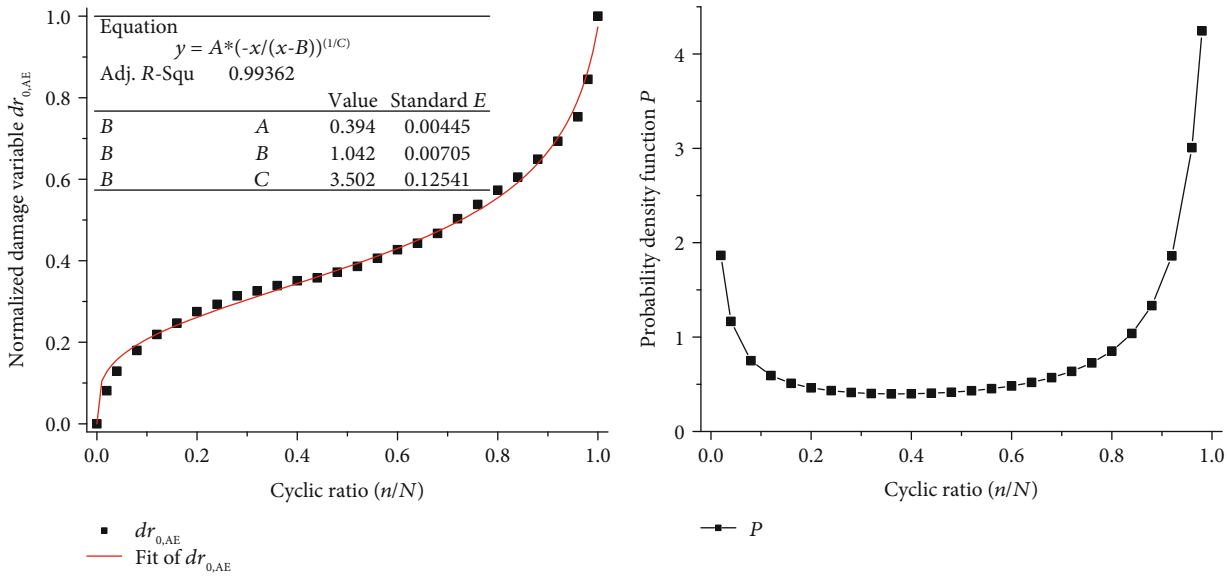

Figure 4: The normalized total damage variable $dr_{0,AE}$ and its probability density function based on AE for concrete. (a) Normalized total damage variable $dr_{0,AE}$ and (b) its probability density function P.

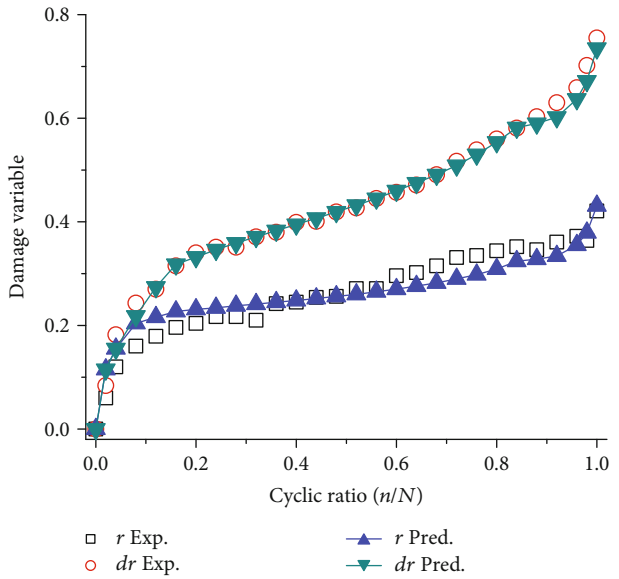

Figure 5: Evolution of fatigue damage variable of concrete.

experimental results. Hence, after obtaining the parameters $dr_{0,AE}(t)$ and $dr_{AE,C}(t)$, the total damage variable $dr(t)$ in the BCM is determined.

Moreover, in order to quantify the fatigue damage and characterize the deterioration behaviors, the irreversible deformation damage variable $r(t)$ is computed by the equations based on the literature [41, 59], such that

$$r(t) = \begin{cases} dr(t), & dr(t) < 0.2, \\ \dfrac{1}{[6 - 5 \cdot dr(t)]}, & dr(t) \geq 0.2. \end{cases} \quad (12)$$

Especially, in a tensile case,

$$r(t) = \frac{[dr(t) - d(t)]}{1 - d(t)}, \quad (13)$$

where

$$d(t) = \begin{cases} 0, & 0 \leq \varepsilon \leq 115.5 \times 10^{-6}, \\ 1 - \left(\dfrac{\varepsilon}{115.5 \times 10^{-6}}\right)^{-1.05}, & \varepsilon > 115.5 \times 10^{-6}, \end{cases} \quad (14)$$

$$dr(t) = d(t) + r(t). \quad (15)$$

The current Young's modulus, irreversible strain [41], residual strain, and fatigue total strain are expressed, respectively, such that

$$E(t) = \sigma_{max} \cdot [\varepsilon - \varepsilon_i(t)]^{-1}, \quad (16)$$

$$\varepsilon_i(t) = r(t) \cdot \varepsilon(t), \quad (17)$$

$$\varepsilon_r(t) = \varepsilon(t) - (\sigma_{max} - \sigma_{min}) \cdot E^{-1}(t), \quad (18)$$

$$\varepsilon_{total}(t) = dr(t) \cdot \varepsilon(t). \quad (19)$$

4. Verification and Discussion

4.1. Three Main Deterioration Behaviors of Plain Concrete. In order to verify the effectiveness of the proposed method, the experimental results of concrete reported in the literature [15] were used in this section. The mixture ratio was designed as cement : sand : aggregate : water : admixture = 457 : 575 : 1248 : 165 : 3.2 (unit: kg/m^3). In detail, the cement is Portland cement with a 28 d strength 47.4 MPa, the water is tap

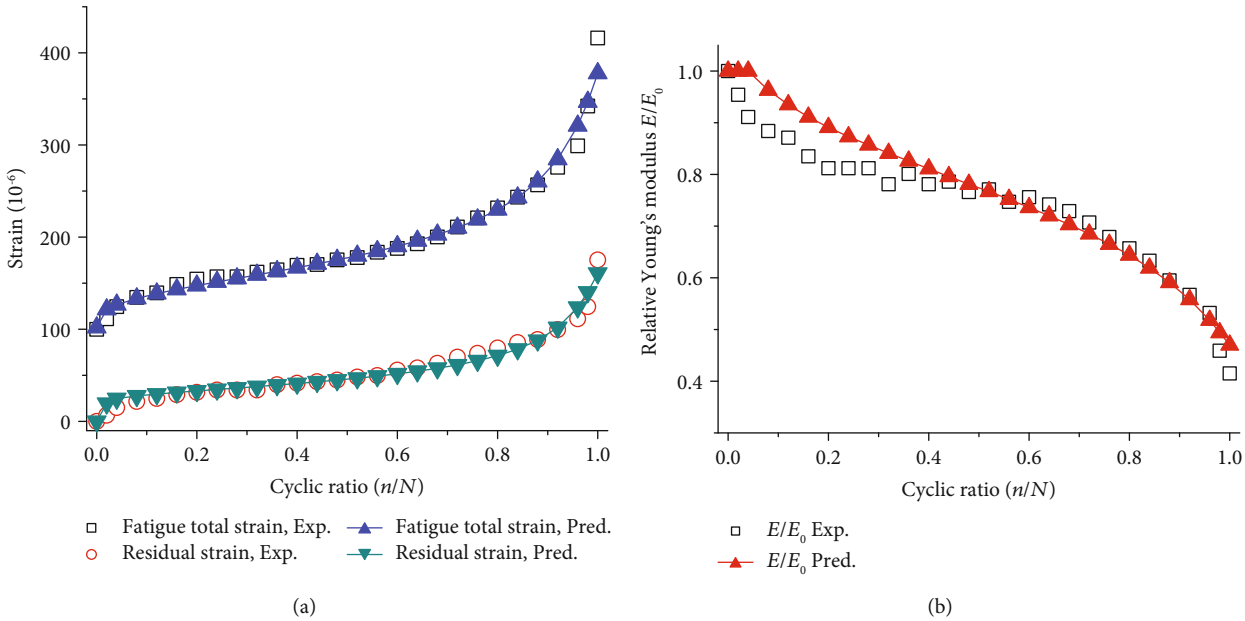

Figure 6: Performance deterioration of concrete under fatigue loading. (a) Strain development. (b) Young's modulus degradation E/E_0.

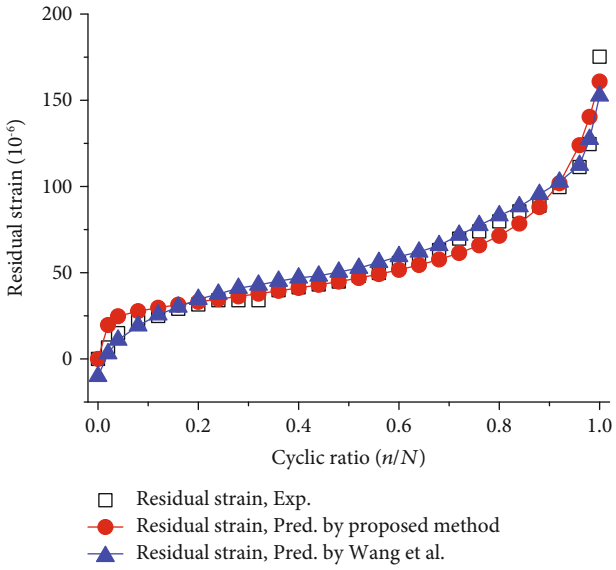

Figure 7: Residual strain development of concrete under fatigue loading.

water, the aggregates are crushed limestone, and the admixture is the superplasticizer. The 28 d strength of concrete is 51.7 MPa. By applying the proposed method, the parameters were calibrated as follows (see Figure 4): $A_1 = 0.394$, $A_2 = 1.042$, $A_3 = 3.502$, $A_4 = 1.774$, and $A_5 = -1.062$. The predicted results of the damage variable are plotted in Figure 5. It reveals that the predicted results agree with the experimental results, and the proposed method is able to capture the mechanisms of damage accumulation.

In addition, by submitting the predicted results of the damage variable into the BCM (equations (12), (15), (16), (17), and (19)), the predictions of the deterioration behaviors are obtained in Figure 6. It illustrates that the predictions of the proposed method agree with the experimental results. In detail, Figure 6(a) shows that the predicted results of fatigue total strain and residual strain coincide with the experimental results. Figure 6(b) expresses that the predicted results of Young's modulus deterioration also agree with the experimental results.

It is noteworthy that the AE method in the literature [15] only considered the characterization of the residual strain of concrete under fatigue loading (see Figure 7) and did not capture the mechanisms of damage accumulation.

4.2. Three Main Deterioration Behaviors of Rubberized Concrete. Furthermore, the experimental results of rubberized concrete reported in the literature [15] were also used to verify the effectiveness of the proposed method. The mixture ratio was designed as cement : sand : aggregate : water : rubber : admixture = 457 : 431 : 1 248 : 165 : 60 : 4.57 (unit: kg/m^3). In detail, the mechanically crushed rubber particles from a waste tire were 2–3 mm in diameter. The 28 d strength rubberized concrete is 38.7 MPa. By applying the proposed method, the parameters were calibrated as follows (see Figure 8): $A_1 = 0.264$, $A_2 = 1.007$, $A_3 = 3.721$, $A_4 = 2.035$, and $A_5 = -1.282$. The predicted results of the damage variable are plotted in Figure 9. It reveals that the predicted results agree with the experimental results, and the proposed method is able to capture the mechanisms of damage accumulation.

The predictions of the deterioration behaviors of rubberized concrete are also obtained in Figure 10, by submitting the predicted results of the damage variable into the BCM (equations (12), (15), (16), (17), and (19)). It shows that the predictions of the proposed method agree with the experimental results. In detail, Figure 10(a) shows that the predicted results of fatigue total strain and residual strain coincide with the experimental results. Figure 10(b)

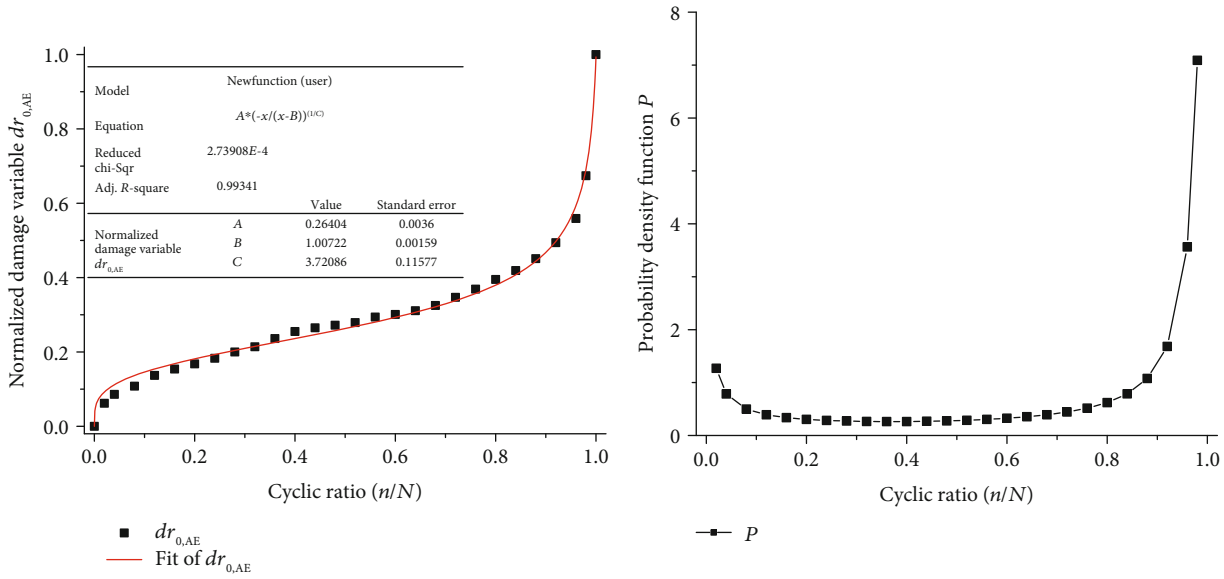

FIGURE 8: The normalized total damage variable $dr_{0,AE}$ and its probability density function based on AE for rubberized concrete. (a) Normalized total damage variable $dr_{0,AE}$ and (b) its probability density function P.

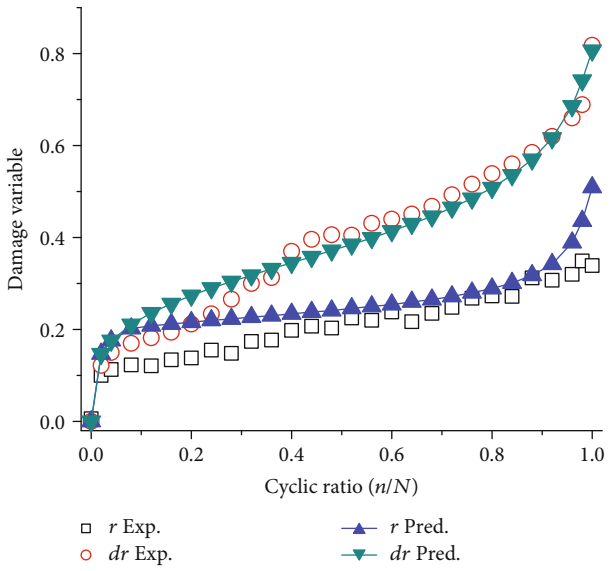

FIGURE 9: Evolution of fatigue damage variable of rubberized concrete.

expresses that the predicted results of Young's modulus deterioration also agree with the experimental results.

Therefore, it is evident that the proposed method is able to quantify the fatigue damage and characterize the deterioration behaviors of concrete under fatigue loading.

4.3. Mechanism of Three-Stage Behaviors. The three-stage behaviors for materials under fatigue loading generally received a number of attentions in fatigue community. For concrete material under fatigue loading, it is found that the total strain and residual strain experience a fast but decelerated increase during the first stage (0–10%) of the lifetime, a slow and smooth increase during the second stage (10–80% of the lifetime), and a fast and accelerated increase during the third stage while the concrete specimens approach macroscopic failure (80–100% of the lifetime) [15, 41, 44, 45, 48]. In addition, the degradation of Young's modulus also experiences a similar three-stage process [15, 41, 45]. It is concluded that these three-stage behaviors are mainly caused by random microcrack initiation, propagation, coalescence, and the development of the macrocrack in the materials. In order to characterize the three-stage behaviors, several mechanisms and theories have been developed by different researches [41, 43, 47].

In this work, based on the researches [41, 47], the three-stage fatigue damage mechanism is proposed as follows.

During the first stage, the most critical defects/cracks are initiated and propagated. The higher the load the larger the number of defects concerned, which explains the rising AE activity. At this stage, the AE signals are due to both initiation of cracks and propagation of initial cracks, which includes both mode-I cracks and irreversible deformation fractures. Especially, the crack behaviors are presumed to be under the regime of both quasistatic and fatigue effects. Between both, the quasistatic effect regime is proposed to play a dominant role in affecting crack behaviors at the beginning, and it is proposed to recede when the loading cycles approach the second stage. Hence, under the regimes, the deterioration behaviors experience a fast but decelerated increase, and the quiet time zone of AE counts occurs in certain conditions during this stage. Furthermore, in this work, the failure of fibers and the fractures of irreversible deformation elements in BCM are utilized to model both initiation and propagation of mode-I cracks and irreversible deformation fractures in this stage, respectively. The proposed damage evolution function with a fast but decelerated increase is able to characterize the behaviors in this stage (Figure 2).

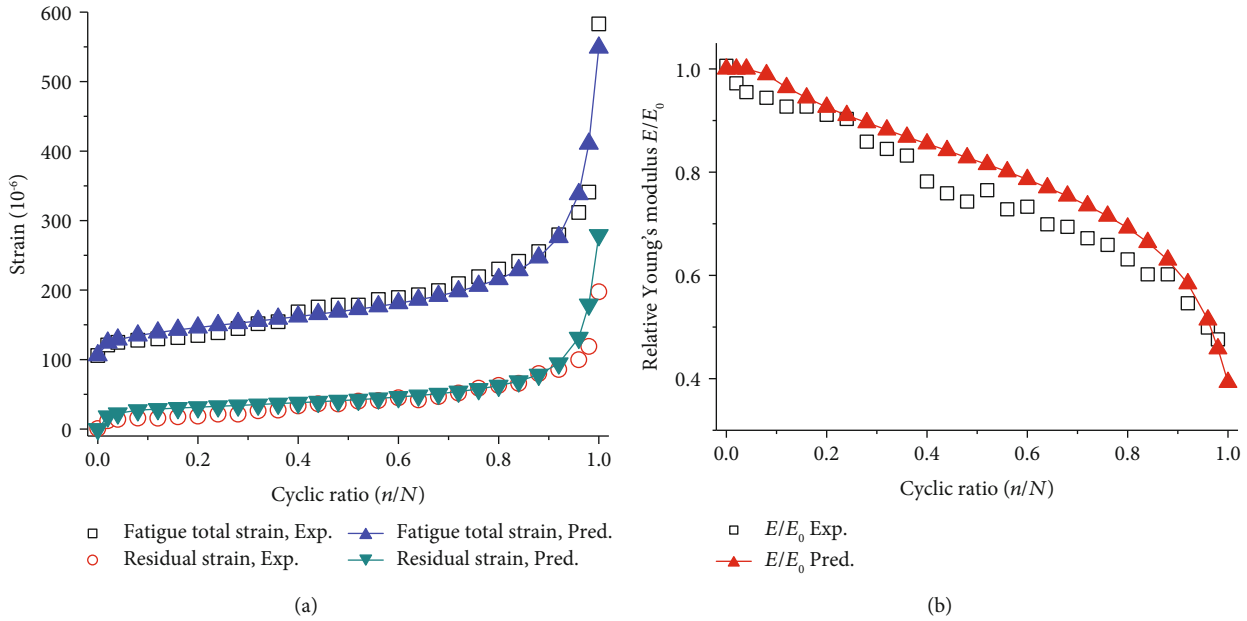

FIGURE 10: Performance deterioration of rubberized concrete under fatigue loading. (a) Strain development and (b) Young's modulus degradation E/E_0.

During the second stage, the rate of the crack initiation decreases, while the rate of the propagation of existing cracks is stable. Hence, the AE counts are experiencing a stable growing process. It illustrates that the regime of the quasi-static effect has been replaced entirely by that of the stable fatigue effect with a stable damage accumulation. Moreover, the fibers and irreversible deformation elements and related evolution function of BCM are verified to be effective to describe the behaviors against experimental results.

During the last stage, the macrocrack initiates due to the coalescence of the microcracks and undergoes an unstable and rapid development until the final failure of the materials. The AE signals are caused by both the propagation of the macrocrack and the initiation and propagation of microcracks in its fracture process zone. The behaviors are concluded as a result of an unstable fatigue failure effect regime. The BCM shows a fast, accelerated, and unstable increase of damage accumulation for characterizing the behaviors.

5. Conclusions

In this work, we developed an AE quantification method of damage in concrete under fatigue loading by combining AE and the BCM. The conclusions are obtained as follows.

The quantification method of damage for concrete under fatigue loading was developed, through establishing a relationship between normalized AE counts and the damage variable based on the BCM.

Additionally, the method is able to characterize the three main deterioration behaviors of concrete, including Young's modulus degradation, fatigue total strain, and residual strain development, simultaneously.

Furthermore, the proposed method was verified against the experimental results. It captures the mechanisms of damage accumulation by combining AE and damage mechanics.

This method applied the AE experimental results in the literature [15] to verify its effectiveness, and it introduced the BCM under fatigue loading [41] to establish the relationship between normalized AE counts and the damage variable. Therefore, it is a new work contributed to AE. It will be adapted in quantifying the fatigue damage of reinforced concrete structures and other materials, for example, cement-asphalt mortar.

Data Availability

All the data used to support the findings of this study are included within the article.

Conflicts of Interest

The authors declare that there is no conflict of interest regarding the publication of this paper.

Acknowledgments

This research was supported by the National Natural Science Foundation of China (grant numbers 51808558, 51820105014, U1434204, 51378506, and 51478478); the Natural Science Foundation of Hunan Province (grant number 2019JJ50800); and the China Energy Investment Corporation (grant number SHGF-18-50).

References

[1] T. F. Drouillard, *Acoustic emission: The first half century (No. RFP-4875; CONF-9410182-1)*, EG and G Rocky Flats, Inc., Golden, CO (United States), 1994, Rocky Flats Plant.

[2] M. Ohtsu, "History and fundamentals," in *Acoustic Emission Testing*, C. U. Grosse and M. Ohtsu, Eds., pp. 11–18, Springer, Berlin, Heidelberg, 2008.

[3] M. N. Noorsuhada, "An overview on fatigue damage assessment of reinforced concrete structures with the aid of acoustic emission technique," *Construction and Building Materials*, vol. 112, pp. 424–439, 2016.

[4] S. Sikdar, P. Mirgal, S. Banerjee, and W. Ostachowicz, "Damage-induced acoustic emission source monitoring in a honeycomb sandwich composite structure," *Composites Part B: Engineering*, vol. 158, no. 1, pp. 179–188, 2019.

[5] S. Sikdar and S. Banerjee, *Structural health monitoring of advanced composites using guided waves*, LAP LAMBERT Academic Publishing Website, 2017.

[6] A. Kundu, M. J. Eaton, S. Al-Jumali, S. Sikdar, and R. Pullin, "Acoustic emission based damage localization in composites structures using Bayesian identification," *Journal of Physics: Conference Series*, vol. 842, p. 012081, 2017.

[7] C.-S. A. Gong, H.-C. Lee, Y.-C. Chuang et al., "Design and implementation of acoustic sensing system for online early fault detection in industrial fans," *Journal of Sensors*, vol. 2018, Article ID 4105208, 15 pages, 2018.

[8] D. Pang, Q. Sui, M. Wang, Y. Sai, R. Sun, and Y. Wang, "Acoustic emission source localization system using fiber Bragg grating sensors and a barycentric coordinate-based algorithm," *Journal of Sensors*, vol. 2018, Article ID 9053284, 8 pages, 2018.

[9] G. Chen, Y. Zhang, R. Huang, F. Guo, and G. Zhang, "Failure mechanism of rock bridge based on acoustic emission technique," *Journal of Sensors*, vol. 2015, Article ID 964730, 11 pages, 2015.

[10] D. G. Aggelis, E. Z. Kordatos, and T. E. Matikas, "Acoustic emission for fatigue damage characterization in metal plates," *Mechanics Research Communications*, vol. 38, no. 2, pp. 106–110, 2011.

[11] A. Kahirdeh, C. Sauerbrunn, H. Yun, and M. Modarres, "A parametric approach to acoustic entropy estimation for assessment of fatigue damage," *International Journal of Fatigue*, vol. 100, pp. 229–237, 2017.

[12] M. Rabiei and M. Modarres, "Quantitative methods for structural health management using in situ acoustic emission monitoring," *International Journal of Fatigue*, vol. 49, pp. 81–89, 2013.

[13] S. Yuyama, Z. W. Li, M. Yoshizawa, T. Tomokiyo, and T. Uomoto, "Evaluation of fatigue damage in reinforced concrete slab by acoustic emission," *NDT & E International*, vol. 34, no. 6, pp. 381–387, 2001.

[14] Y. Qiao, W. Sun, and J. Jiang, "Damage process of concrete subjected to coupling fatigue load and freeze/thaw cycles," *Construction and Building Materials*, vol. 93, pp. 806–811, 2015.

[15] C. Wang, Y. Zhang, and A. Ma, "Investigation into the fatigue damage process of rubberized concrete and plain concrete by AE analysis," *Journal of Materials in Civil Engineering*, vol. 23, no. 7, pp. 953–960, 2011.

[16] T. Shiotani, H. Ohtsu, S. Momoki, H. K. Chai, H. Onishi, and T. Kamada, "Damage evaluation for concrete bridge deck by means of stress wave techniques," *Journal of Bridge Engineering*, vol. 17, no. 6, pp. 847–856, 2012.

[17] M. Ohtsu and H. Watanabe, "Quantitative damage estimation of concrete by acoustic emission," *Construction and Building Materials*, vol. 15, no. 5-6, pp. 217–224, 2001.

[18] T. Suzuki and M. Ohtsu, "Quantitative damage evaluation of structural concrete by a compression test based on AE rate process analysis," *Construction and Building Materials*, vol. 18, no. 3, pp. 197–202, 2004.

[19] S. T. Dai and J. F. Labuz, "Damage and failure analysis of brittle materials by acoustic emission," *Journal of Materials in Civil Engineering*, vol. 9, no. 4, pp. 200–205, 1997.

[20] F. T. Peirce, "Tensile test for cotton yarns—the weakest link," *Journal of the Textile Institute Transactions*, vol. 17, pp. T355–T368, 1926.

[21] H. E. Daniels, "The statistic theory of the strength of bundles of threads: I," *Proceedings of the Royal Society of London A*, vol. 183, pp. 405–435, 1945.

[22] L. Mishnaevsky Jr. and P. Brøndsted, "Micromechanical modeling of damage and fracture of unidirectional fiber reinforced composites: a review," *Computational Materials Science*, vol. 44, no. 4, pp. 1351–1359, 2009.

[23] S. Pradhan, A. Hansen, and B. K. Chakrabarti, "Failure processes in elastic fiber bundles," *Reviews of Modern Physics*, vol. 82, no. 1, pp. 499–555, 2010.

[24] F. Raischel, F. Kun, and H. J. Herrmann, "Failure process of a bundle of plastic fibers," *Physical Review E*, vol. 73, no. 6, 2006.

[25] F. Kun, R. C. Hidalgo, F. Raischel, and H. J. Herrmann, "Extension of fibre bundle models for creep rupture and interface failure," *International Journal of Fracture*, vol. 140, no. 1-4, pp. 255–265, 2006.

[26] F. Kun, F. Raischel, R. C. Hidalgo, and H. J. Herrmann, "Extensions of fibre bundle models," in *Modelling critical and catastrophic phenomena in geoscience: a statistical physics approach*, Lecture Notes in Physics, P. Bhattacharyya and B. K. Chakrabarti, Eds., Springer, Berlin, 2006.

[27] J.-L. Le, Z. P. Bažant, and M. Z. Bazant, "Unified nanomechanics based probabilistic theory of quasibrittle and brittle structures: I. Strength, static crack growth, lifetime and scaling," *Journal of the Mechanics and Physics of Solids*, vol. 59, no. 7, pp. 1291–1321, 2011.

[28] X. Ren and J. Li, "Hysteretic deteriorating model for quasi-brittle materials based on micromechanical damage approach," *International Journal of Non-Linear Mechanics*, vol. 46, no. 1, pp. 321–329, 2011.

[29] J. Chen, W. F. Bai, S. L. Fan, and G. Lin, "Statistical damage model for quasi-brittle materials under uniaxial tension," *Journal of Central South University of Technology*, vol. 16, no. 4, pp. 669–676, 2009.

[30] Z. Shan and Z. Yu, "A fiber bundle-plastic chain model for quasi-brittle materials under uniaxial loading," *Journal of Statistical Mechanics: Theory and Experiment*, vol. 2015, no. 11, article P11010, 2015.

[31] G. Hu, J. Liu, L. Graham-Brady, and K. T. Ramesh, "A 3D mechanistic model for brittle materials containing evolving flaw distributions under dynamic multiaxial loading," *Journal of the Mechanics and Physics of Solids*, vol. 78, pp. 269–297, 2015.

[32] A. Burr, F. Hild, and F. A. Leckie, "Micro-mechanics and continuum damage mechanics," *Archive of Applied Mechanics*, vol. 65, no. 7, pp. 437–456, 1995.

[33] J. Mazars and G. Pijaudier-Cabot, "Continuum damage theory – application to concrete," *Journal of Engineering Mechanics*, vol. 115, no. 2, pp. 345–365, 1989.

[34] D. Halm and A. Dragon, "An anisotropic model of damage and frictional sliding for brittle materials," *European Journal of Mechanics - A/Solids*, vol. 17, no. 3, pp. 439–460, 1998.

[35] A. Dragon, D. Halm, and T. Desoyer, "Anisotropic damage in quasi-brittle solids: modelling, computational issues and

applications," *Computer Methods in Applied Mechanics and Engineering*, vol. 183, no. 3-4, pp. 331–352, 2000.

[36] J.-L. Le and Z. P. Bažant, "Unified nano-mechanics based probabilistic theory of quasibrittle and brittle structures: II. Fatigue crack growth, lifetime and scaling," *Journal of the Mechanics and Physics of Solids*, vol. 59, no. 7, pp. 1322–1337, 2011.

[37] Z. Yu, Z. Shan, Z. Ouyang, and F. Guo, "A simple damage model for concrete considering irreversible mode-II microcracks," *Fatigue & Fracture of Engineering Materials & Structures*, vol. 39, no. 11, pp. 1419–1432, 2016.

[38] Z. W. Yu, S. Tan, Z. Shan, and X. Q. Tian, "X-ray computed tomography quantification of damage in concrete under compression considering irreversible mode-II microcracks," *Fatigue & Fracture of Engineering Materials & Structures*, vol. 40, no. 12, pp. 1960–1972, 2017.

[39] J. Najar, "Brittle residual strain and continuum damage at variable uniaxial loading," *International Journal of Damage Mechanics*, vol. 3, no. 3, pp. 260–276, 1994.

[40] X. Q. Feng and D. Gross, "Three-dimensional micromechanical model for quasi-brittle solids with residual strains under tension," *International Journal of Damage Mechanics*, vol. 9, no. 1, pp. 79–110, 2000.

[41] Z. Yu, Z. Shan, and J. Mao, "Fatigue deterioration of quasi-brittle materials," *International Journal of Fatigue*, vol. 118, pp. 185–191, 2019.

[42] D. Sánchez-Molina, E. Martínez-González, J. Velázquez-Ameijide, J. Llumà, M. C. R. Soria, and C. Arregui-Dalmases, "A stochastic model for soft tissue failure using acoustic emission data," *Journal of the Mechanical Behavior of Biomedical Materials*, vol. 51, pp. 328–336, 2015.

[43] L. Susmel, "A unifying methodology to design un-notched plain and short-fibre/particle reinforced concretes against fatigue," *International Journal of Fatigue*, vol. 61, pp. 226–243, 2014.

[44] J.-K. Kim and Y.-Y. Kim, "Experimental study of the fatigue behavior of high strength concrete," *Cement and Concrete Research*, vol. 26, no. 10, pp. 1513–1523, 1996.

[45] P. B. Cachim, J. A. Figueiras, and P. A. A. Pereira, "Fatigue behavior of fiber-reinforced concrete in compression," *Cement and Concrete Composites*, vol. 24, no. 2, pp. 211–217, 2002.

[46] A. Berkovits and D. Fang, "Study of fatigue crack characteristics by acoustic emission," *Engineering Fracture Mechanics*, vol. 51, no. 3, pp. 401–416, 1995.

[47] F. Thummen, C. Olagnon, and N. Godin, "Cyclic fatigue and lifetime of a concrete refractory," *Journal of the European Ceramic Society*, vol. 26, no. 15, pp. 3357–3363, 2006.

[48] V. M. Kindrachuk, M. Thiele, and J. F. Unger, "Constitutive modeling of creep-fatigue interaction for normal strength concrete under compression," *International Journal of Fatigue*, vol. 78, pp. 81–94, 2015.

[49] C. Sauerbrunn, A. Kahirdeh, H. Yun, and M. Modarres, "Damage assessment using information entropy of individual acoustic emission waveforms during cyclic fatigue loading," *Applied Sciences*, vol. 7, no. 6, p. 562, 2017.

[50] T. M. Roberts and M. Talebzadeh, "Fatigue life prediction based on crack propagation and acoustic emission count rates," *Journal of Constructional Steel Research*, vol. 59, no. 6, pp. 679–694, 2003.

[51] Z. Han, H. Luo, Y. Zhang, and J. Cao, "Effects of microstructure on fatigue crack propagation and acoustic emission behaviors in a micro-alloyed steel," *Materials Science and Engineering A*, vol. 559, pp. 534–542, 2013.

[52] P. A. Vanniamparambil, I. Bartoli, K. Hazeli et al., "An integrated structural health monitoring approach for crack growth monitoring," *Journal of Intelligent Material Systems and Structures*, vol. 23, no. 14, pp. 1563–1573, 2012.

[53] P. A. Vanniamparambil, U. Guclu, and A. Kontsos, "Identification of crack initiation in aluminum alloys using acoustic emission," *Experimental Mechanics*, vol. 55, no. 5, pp. 837–850, 2015.

[54] D. G. Aggelis, E. Z. Kordatos, and T. E. Matikas, "Monitoring of metal fatigue damage using acoustic emission and thermography," *Journal of Acoustic Emission*, vol. 29, 2011.

[55] P. H. Ziehl, *Development of a damage based design criterion for fiber reinforced vessels*, The University of Texas, Texas, 2000.

[56] RILEM Technical Committee (Masayasu Ohtsu), "Recommendation of RILEM TC 212-ACD: acoustic emission and related NDE techniques for crack detection and damage evaluation in concrete," *Materials and Structures*, vol. 43, no. 9, pp. 1187–1189, 2010.

[57] M. Ohtsu, T. Isoda, and Y. Tomoda, "Acoustic emission techniques standardized for concrete structures," *Journal of Acoustic Emission*, vol. 25, pp. 21–32, 2007.

[58] S. G. Shah and J. M. C. Kishen, "Use of acoustic emissions in flexural fatigue crack growth studies on concrete," *Engineering Fracture Mechanics*, vol. 87, pp. 36–47, 2012.

[59] J. F. Sima, P. Roca, and C. Molins, "Cyclic constitutive model for concrete," *Engineering Structures*, vol. 30, no. 3, pp. 695–706, 2008.